Enhanced nutrient uptake is sufficient to drive emergent cross-feeding between bacteria

Ryan K Fritts[1], Jordan T Bird[2,3], Megan G Behringer[4], Anna Lipzen[5], Joel Martin[5] Michael Lynch[4], and James B McKinlay[1]*

[1]Department of Biology, Indiana University Bloomington, Bloomington, IN, 47405

[2]Department of Biochemistry and Molecular Biology, University of Arkansas for Medical Sciences, Little Rock, AR, 72205

[3]Arkansas Children's Research Institute, Little Rock, AR, 72205

[4]School of Life Sciences, Biodesign Center for Mechanisms of Evolution, Arizona State University, Tempe, AZ, 85281

[5]Department of Energy Joint Genome Institute, Walnut Creek, CA, 94598

*Corresponding author

Phone: 812-855-0359

Email: jmckinla@indiana.edu

Running title. Bacterial cross-feeding driven by enhanced nutrient uptake.

Keywords: cross-feeding, bacteria, coculture, nutrient, metabolic

The authors declare no conflict of interest.

Abstract

Interactive microbial communities are ubiquitous on Earth. Within microbial communities, nutrient exchange, also called cross-feeding, is widespread. Cross-feeding is thought to arise from the need to satisfy nutrient requirements of recipient microbes, in many cases with producer microbes excreting costly, communally valuable metabolites such as vitamins, amino acids, or ammonium. However, we possess an incomplete understanding of the genetic basis and molecular mechanisms by which cross-feeding of communally valuable metabolites evolves. Previously we engineered a mutualistic cross-feeding relationship between N_2-fixing *Rhodopseudomonas palustris* and fermentative *Escherichia coli*. In this synthetic mutualism, genetically engineered *R. palustris* excretes essential nitrogen in the form of ammonium to *E. coli*, while *E. coli* excretes essential carbon in the form of fermentation products to *R. palustris*. Here, we used the same species, but with a wildtype strain of *R. palustris* not known to excrete ammonium, to enrich for a nascent cross-feeding relationship. We found that emergent ammonium cross-feeding relies not on a mutation in the producer *R. palustris* but rather a single missense mutation in the recipient *E. coli.* This mutation in *E. coli* NtrC, the master regulator of nitrogen scavenging, results in constitutive activation of an ammonium transporter and likely allows *E. coli* to subsist on the small amount of ammonium that leaks from WT *R. palustris* and reciprocate through the excretion of organic acids. Overall, our results indicate that enhanced nutrient uptake by recipients, rather than increased excretion by producers, is a plausible and possibly prevalent mechanism by which cross-feeding interactions emerge.

Significance

Microbial communities orchestrate biogeochemical cycles and can cause or prevent polymicrobial infections. Interactions between microbes, including nutrient cross-feeding, can determine which species successfully colonize and thrive in a given niche. Here, we demonstrate that within a cross-feeding relationship, recipients, rather than producers, can drive the evolutionary emergence of nutrient exchange. In this case, the recipient bacterium drives emergent ammonium cross-feeding by enhancing nutrient uptake via upregulation of nitrogen acquisition genes. Our findings show that microbial species can rapidly adapt to coexist by exchanging nutrients and that the recipient species play an underappreciated role in driving the emergence of cross-feeding interactions.

Introduction

Microorganisms typically exist as members of diverse and highly interactive communities wherein nutrient exchange, also known as cross-feeding, is thought to be ubiquitous (1-7). The prevalence of cross-feeding interactions may explain, in part, why many microbial species are unable to synthesize particular essential metabolites such as vitamins and amino acids (i.e. auxotrophy), and therefore must acquire these compounds, often from other community members (1, 7, 8). Furthermore, microbes in nature experience varying degrees of starvation and often exist in states of low metabolic activity (9, 10) and cross-feeding might serve as an important way by which limiting nutrients are acquired. However, elucidating the genetic basis of emergent

cross-feeding interactions and tracking their evolutionary dynamics within natural microbial communities is difficult due to their sheer complexity. To overcome the intrinsic complexities of natural microbial communities, tractable synthetic consortia have proven useful as model systems for studying assorted aspects of the mechanisms, ecology, and evolution of microbial communities and for biotechnological applications (4, 11-16).

To study the molecular mechanisms of nutrient cross-feeding, we previously developed a synthetic bacterial coculture in which *Escherichia coli* and *Rhodopseudomonas palustris* reciprocally exchange essential metabolites under anaerobic conditions (Fig.1A) (17-20). In this coculture, *E. coli* ferments glucose, a carbon source that *R. palustris* cannot consume, and excretes ethanol and organic acids as waste products. The organic acids, with the exception of formate, serve as the sole carbon sources for *R. palustris* (Fig. 1A). In return, *R. palustris* fixes dinitrogen gas (N_2) via the enzyme nitrogenase and excretes ammonium (NH_4^+), which is the sole nitrogen source for *E. coli* (Fig. 1A). Because both species depend on essential nutrients provided by their partner species, this coculture functions as an obligate mutualism.

NH_4^+ cross-feeding from *R. palustris* to *E. coli* is thought to depend on the equilibrium between NH_3 and NH_4^+. The small proportion of NH_3 present in neutral pH environments is membrane permeable and can diffuse out of cells (21, 22). Leaked NH_4^+ can be recaptured by AmtB transporters (21), which in the case of *R. palustris* helps avoid loss of valuable NH_4^+ (Fig. 1B) (17, 18). NH_4^+ leakage is also limited through the strict regulation of N_2 fixation, including by the transcriptional activator NifA,

so that energetically expensive N_2 fixation is only performed when preferred nitrogen sources such as NH_4^+ are limiting (23). Previously, we identified two types of mutations that increase NH_4^+ excretion by *R. palustris* during N_2 fixation and support coculture growth with *E. coli* (17): (i) deletion of *amtB*, which prevents recapture of leaked NH_3, or (ii) a 48-bp deletion within *nifA* (denoted as NifA*), which locks NifA into an active conformation (24) (Fig. 1B). In contrast, wildtype (WT) *R. palustris* does not readily support coculture growth with *E. coli* due to insufficient NH_4^+ excretion (17).

While mutualistic cross-feeding of communally valuable NH_4^+ between *E. coli* and *R. palustris* can be rationally engineered, it remained to be seen whether such an interaction could arise spontaneously. Herein we experimentally evolved cocultures pairing *E. coli* with WT *R. palustris* for ~146 generations. While a nascent mutualism was established and growth trends improved over serial transfers, growth and metabolic trends remained distinct from those of both ancestral and parallel evolved cocultures of *E. coli* and *R. palustris* NifA*. By pairing ancestral and evolved isolates of each species in coculture, we determined that adaptation by *E. coli* was solely responsible for establishing a mutualism with WT *R. palustris*. Whole-genome sequencing and subsequent genetic verification identified a single missense mutation in the *E. coli* transcriptional activator for nitrogen starvation, NtrC, that was sufficient for establishing mutualistic growth with WT *R. palustris*. This mutation results in constitutive AmtB expression, presumably enhancing NH_4^+ uptake. Our results suggest that mutations that improve acquisition of communally valuable nutrients by recipient species are favored to evolve and can promote the emergence of stable cross-feeding interactions within synthetic consortia, and potentially in natural communities.

Results

Mutualistic cross-feeding between wildtype *R. palustris* and *E. coli* can spontaneously evolve. We confirmed our previous observations (17) that WT *R. palustris* exhibits undetectable NH_4^+ excretion and does not readily support coculture growth with WT *E. coli*, in stark contrast to an engineered NifA* mutant strain, which excretes NH_4^+ and readily supports coculture growth (Fig. 1C and D). Whereas cocultures with *R. palustris* NifA* (NifA*-based cocultures) grew to an optical density (OD_{660}) > 2.0 in 4-6 days with a doubling time of ~12 h, cocultures with WT *R. palustris* (WT-based cocultures) did not exhibit appreciable growth in the same time frame (Fig. 1D). However, we hypothesized that prolonged incubation might enrich for spontaneous mutants that permit coculture growth. After 50 days, WT-based cocultures indeed reached optical densities similar to those observed for NifA*-based cocultures, albeit with a doubling time of ~13 days (Fig. 1D).

Upon establishing a spontaneously evolved nascent mutualism between WT *R. palustris* and *E. coli*, we experimentally evolved six replicates of both WT-based cocultures (A-F) and NifA*-based cocultures (M-R), all with WT *E. coli* (Fig. 2A), to compare their stability, evolutionary trajectory, and species and genotypic composition. Cocultures were serially transferred 25 times, corresponding to ~146 generations, with ~5.6 generations estimated per serial coculture (including the original cocultures designated, transfer 0) based on the 1:50 dilution used for each transfer. We then revived cocultures from frozen stocks at an early (transfer 2; generation 17) and later (transfer 25; generation 146) time point to compare growth and population trends. We tracked the growth of revived cocultures until stationary phase, i.e., an OD_{660} >2 and a

low metabolic rate based on H_2 measurements. At generation 17 (G17), NifA*-based cocultures exceeded an OD_{660} of 2 in under 8 days whereas WT-based cocultures took ~40 days (Fig. 2B). By generation 146 (G146), the time needed to reach OD_{660} > 2 had decreased for every lineage (Fig. 2C). The shortened growth phase was most pronounced for WT-based cocultures, which all reached OD_{660} > 2 in under 17 days by G146, less than half the time needed at G17 (Fig. 2B, C); WT-based coculture doubling times decreased from 135 ± 55 h to 47 ± 10 h (Fig. 2D). Though less drastic, NifA*-based coculture doubling times also decreased, in this case from ~11 h to ~8 h (Fig. 2D). Thus, WT *R. palustris* and *E. coli* adapted to grow better together, although this pairing never grew as fast as unevolved engineered NifA*-based cocultures.

Because growth trends differed between WT-based cocultures and NifA*-based cocultures, we wondered how the levels of each species were affected. We therefore enumerated viable cells as colony forming units (CFUs) on selective agar for each species at the final time points for G17 and G146 cocultures shown in Fig. 2A and B. At G17, both *R. palustris* and *E. coli* populations in WT-based cocultures were lower than those in NifA*-based cocultures (Fig. 3A). It is worth noting that NifA*-based cocultures were plated after ~10 days, whereas WT-based cocultures were plated after 39-43 days due to their slower growth rate. Consequently, the background death rate during the additional ~30 days of slower growth for WT-based cocultures could have contributed to the lower final CFUs. At G146, *R. palustris* abundances in WT-based cocultures had increased >14-fold and exceeded *R. palustris* abundances observed in NifA*-based cocultures by ~2-fold (Fig. 3). *E. coli* abundances in WT-based cocultures also increased >7-fold by G146, but not to abundances observed in NifA*-based cocultures

(Fig. 3). Due to the disproportionate increase in each population in WT-based cocultures between G17 and G146, *E. coli* percentages remained low at 1-5%, relative to 11-21% in NifA*-based cocultures (Fig. 3B). These differences in *E. coli* populations between WT- and NifA*-based cocultures are consistent with previous findings that higher levels of NH_4^+ excretion by *R. palustris* support faster growth and higher *E. coli* abundances (17-19).

In contrast to WT-based cocultures, NifA*-based cocultures did not display higher cell densities for either species at G146 compared to G17 (Fig. 3). For *E. coli*, the average densities were 4.7×10^8 CFUs/ml and 6.9×10^8 CFUs/ml at G17 and G146, respectively. For *R. palustris*, the average densities were 3.4×10^9 CFUs/ml and 3.9×10^9 CFUs/ml at G17 and G146, respectively. The average *E. coli* percentage in NifA*-based cocultures was similar at G17 (16.5%) and at G146 (16.4%) (Wilcoxon matched-pairs signed rank test, P=0.563).

Metabolic differences between WT-based and NifA*-based cocultures help explain growth and population trends. Our previous *R. palustris* and *E. coli* coculture studies demonstrated that growth and population trends can be strongly influenced by cross-feeding levels of both NH_4^+ and organic acids (17-19). Therefore, we quantified glucose consumption and fermentation product yields for cocultures at G17 and G146 at stationary phase. At G17, glucose consumption by *E. coli* in WT-based cocultures was about half of that in NifA*-based cocultures (Fig. 4A). The lower glucose consumption in WT-based cocultures can explain in part the lower CFUs observed in Fig. 3A. Previously, we showed that non-growing *E. coli* can ferment glucose, and that this growth-independent fermentation can provide sufficient carbon to support *R. palustris*

growth (19). We hypothesize that growth-independent fermentation by *E. coli* was an important cross-feeding mechanism during the extremely slow growth of early WT-based cocultures. By G146, *E. coli* consumed similar concentrations of glucose as NifA*-based cocultures in three WT-based coculture lineages, with one lineage consuming more glucose (Fig. 4A). The general increase in glucose consumption by *E. coli* in WT-based cocultures from G17 to G146 (Fig. 4A) is associated with both faster coculture doubling times (Fig. 2D) and higher *E. coli* abundances (Fig. 3B).

We also observed a potential trade-off between coculture growth rate and coculture growth yield (ΔOD_{660} / glucose consumed). For example, WT-based G17 cocultures had the slowest growth rates but highest growth yields, whereas NifA*-based G146 cocultures had the fastest growth rates but lowest growth yields (Fig. 4B). Trade-offs between growth rate and yield have been reported in multiple microbial species under various conditions (25-27). In our case, the metabolic trends point to possible explanations for the apparent trade-off. For example, formate produced by *E. coli* is not consumed by *R. palustris* and thus typically accumulates in cocultures (17). However, no formate was detected in WT-based G17 cocultures and yields were approximately half of that for NifA*-based cocultures at G146 (Fig. 4C). Low formate yields could be explained in part by increased conversion of formate to H_2 and CO_2 by the *E. coli* formate hydrogenlyase (28, 29). Consistent with this possibility, WT-based cocultures had higher H_2 yields at G17 and G146 (Fig. 4D). Low formate yields could also be explained by decreased formate production by *E. coli* in favor of other fermentation products that *R. palustris* can readily consume. We previously observed low formate yields in slow-growing, nitrogen-limited NifA*-based cocultures (19, 20), suggesting that

formate production by *E. coli* varies in response to growth rate. We have also not ruled out the possibility that *R. palustris* can consume some formate under certain conditions. In addition to formate, consumable organic acid yields were also lower at both G17 and G146 WT-based cocultures relative to NifA*-based cocultures (Fig. S2). Organic acid accumulation in cocultures can acidify the medium to inhibitory levels (17) . At both G17 and G146, the lower yields of formate and other organic acids in WT-based cocultures translated into higher pH values than in NifA*-based cocultures (Fig. 4E). This lower level of acidification combined with the likelihood of a higher proportion of glucose being fermented into consumable organic acids rather than formate could explain the higher *R. palustris* cell densities at G146 in WT-based cocultures compared to NifA*-based cocultures (Fig. 3B).

A single mutation in an *E. coli* nitrogen starvation response regulator is sufficient for mutualistic growth with WT *R. palustris*. We hypothesized that the growth of WT-based cocultures was due to adaptive mutations in one or both species. To determine whether the evolution of either or both species was necessary to establish a nascent mutualism, we isolated single colonies of each species from ancestral WT populations and evolved G146 cocultures and paired them in all possible combinations (Fig. 5A). Only those pairings featuring evolved *E. coli* grew to an OD_{660} >0.5 after ~24 days (Fig. 5B). Cocultures pairing evolved *E. coli* with ancestral or evolved WT *R. palustris* exhibited similar doubling times of ~67 h (Fig. S1). These results indicate that adaptation by *E. coli* alone is sufficient to establish a nascent mutualism with WT *R. palustris*. Accordingly, we did not observe increased NH_4^+ excretion in evolved WT *R. palustris* N_2-fixing monocultures compared to the ancestral strain (Fig. S1).

To identify candidate mutations in *E. coli* that could enable coculture growth, we sequenced the genomes of populations in all six WT-based coculture lineages after 138-143 generations. Multiple mutations were identified in each species of each experimental line at varying frequencies (Supplemental Files 1 and 2). Consistent with the relatively slow growth rates of WT-based cocultures (Fig. 5B), we did not detect any *nifA* nor *amtB* mutations in evolved WT *R. palustris* populations, which would enable rapid coculture growth. In *E. coli*, we identified the same fixed missense mutation in *glnG* (henceforth called *ntrC*) in all evolved WT-based cocultures lineages at G146, replacing serine 163 with an arginine within the AAA+ domain in the encoded the response regulator NtrC ($NtrC^{S163R}$, Fig. 5C). NtrC and the histidine kinase NtrB form a two-component system that senses and coordinates the nitrogen starvation response in *E. coli* (30, 31). Our lab previously found that the *E. coli* NtrBC-regulon is highly expressed in coculture with *R. palustris* NifA* (20). Thus *E. coli* NtrBC might be even more important in coculture with WT *R. palustris* wherein *E. coli* nitrogen starvation is expected to be intensified. Subsequent sequencing of populations from generation 11 revealed that the $NtrC^{S163R}$ mutation was enriched early in the evolution of WT-based cocultures (Table S1). The $NtrC^{S163R}$ mutation was also enriched in WT-based cocultures evolved under static conditions (Table S1), suggesting that the mutation was also adaptive in spatially heterogenous environments. Further, we also identified multiple, though different, high frequency mutations in *ntrBC* in *E. coli* populations from NifA*-based cocultures evolved under both well-mixed and static conditions (Table S1), suggesting that mutations affecting nitrogen scavenging are also adaptive in the

248 presence of an NH_4^+-excreting partner. All of these observations strongly suggest the
249 adaptive importance of *E. coli* NtrBC mutations like NtrC^{S163R} for coculture growth.

250 To determine if the NtrC^{S163R} mutation alone was sufficient to support coculture
251 growth with WT *R. palustris,* we moved the NtrC^{S163R} allele into the ancestral *E. coli*
252 strain. Cocultures pairing *E. coli* NtrC^{S163R} with WT *R. palustris* grew with a doubling
253 time of 124 ± 22 h, approximately twice as long as cocultures with evolved *E. coli*
254 isolates, but much faster than cocultures with ancestral *E. coli* (Fig. 6A). Thus, the
255 NtrC^{S163R} mutation is sufficient to drive coculture growth. Cocultures with *E. coli*
256 NtrC^{S163R} reached similar final cell densities, but supported lower WT *R. palustris*
257 abundances than cocultures with evolved *E. coli* isolates (Fig. 6B). We speculate that
258 some of the additional mutations present in evolved *E. coli* isolates (Supplemental Files
259 1 and 2) are adaptive under coculture conditions and may account for the faster growth
260 rate and higher densities of *R. palustris* in these cocultures (Fig. 6A and B). Because of
261 the striking parallelism of the NtrC^{S163R} mutation across coculture lineages, we
262 wondered if it might have been prevalent in the ancestral population. We therefore
263 examined ten ancestral *E. coli* isolates that underwent 35 days of coculture growth with
264 WT *R. palustris* (Fig. 6A) for the NtrC^{S163R} mutation. All ten isolates had the WT *ntrC*
265 allele. Thus, if the NtrC^{S163R} mutation is in the *E. coli* ancestral population it is at a low
266 frequency.

267 **The NtrC^{S163R} allele constitutively activates expression of the ammonium**
268 **transporter AmtB in *E. coli.*** Based on the effects of NtrC mutations observed by
269 others (32, 33), we hypothesized the NtrC^{S163R} allele enables coculture growth with WT
270 *R. palustris* by conferring constitutive expression of NtrBC-regulated genes important for

NH_4^+ acquisition. We previously determined that NtrC and AmtB were crucial gene products within the NtrBC regulon for growth and coexistence with *R. palustris* NifA* (18, 20). To test if the $NtrC^{S163R}$ allele increased *amtB* and *ntrC* expression, we measured transcript levels by reverse transcription quantitative PCR (RT-qPCR) in *E. coli* monocultures grown with 15 mM NH_4Cl or subjected to complete nitrogen starvation (~10 h with 0 mM NH_4Cl). We chose to perform RT-qPCR on *E. coli* monocultures, because ancestral WT *E. coli* does not readily grow with WT *R. palustris* and because *E. coli* typically constitutes a low percentage (1-5%) of WT-based cocultures, meaning most mRNA in cocultures would be from *R. palustris*.

When cultured with NH_4Cl, the *E. coli* $NtrC^{S163R}$ mutant exhibited ~30 and ~15-fold higher expression of *amtB* and *ntrC*, respectively, than WT *E. coli* (Fig. 6C). This result is consistent with our hypothesis that the $NtrC^{S163R}$ allele constitutively activates expression of its regulon. Following 10 h of nitrogen starvation, we saw similarly high *amtB* and *ntrC* expression by both the WT and the $NtrC^{S163R}$ strains (Fig. 6C). Thus, both the WT and $NtrC^{S163R}$ *E. coli* strains are able to commence strong transcriptional responses to extreme nitrogen starvation. We expect that the level of nitrogen limitation experienced by *E. coli* in coculture with WT *R. palustris* is less extreme than the complete nitrogen starvation conditions used in our qPCR experiments. Although we cannot detect NH_4^+ excretion by WT *R. palustris*, the equilibrium with NH_3 dictates that some will be excreted, possibly within the nM to low µM range where AmtB is critically important (21). We also know that AmtB is important in coculture for *E. coli* to compete for transiently available NH_4^+ that *R. palustris* will otherwise reacquire (18). We therefore hypothesize that the $NtrC^{S163R}$ mutation primes *E. coli* for coculture growth with *R.*

palustris, by maintaining high AmtB expression, thereby enabling acquisition of scarcely available NH_4^+. The *E. coli* growth that results from NH_4^+ acquisition then fuels a higher rate of reciprocation through the excretion of organic acids, allowing a mutualism to emerge.

Discussion

Here, we determined that in cocultures requiring nitrogen transfer from *R. palustris to E. coli*, an *E. coli* $NtrC^{S163R}$ mutation alone is sufficient to enable coculture growth. The $NtrC^{S163R}$ allele results in constitutive activity of the transcriptional activator NtrC and thus increased expression of the AmtB NH_4^+ transporter, which we hypothesize enhances NH_4^+ uptake. This is the first mutation we have identified in the NH_4^+ recipient species *E. coli* that is sufficient to support mutualistic coculture growth with WT *R. palustris*. Overall, our data suggest that a recipient species can establish cross-feeding interactions through enhanced nutrient uptake.

Our previous work on this synthetic cross-feeding consortium utilized *R. palustris* NifA* and ΔAmtB strains that we engineered to excrete NH_4^+ and foster coculture growth (17-19). In the present study, we did not identify any *nifA* or *amtB* mutations in evolved WT *R. palustris* populations. This suggests that although the NifA*-based cocultures exhibit more rapid coculture growth than WT-based cocultures, *R. palustris nifA* and *amtB* mutations likely incur a fitness cost, such as an increased energetic burden of constitutive nitrogenase expression due to the NifA* mutation, or loss of NH_4^+ to WT competitors in the case of an inactivating *amtB* mutation. However, it does not appear that *R. palustris* NifA* regained regulation of nitrogenase and limited NH_4^+ excretion during the experimental evolution. Instead, evolved NifA*-based cocultures

317 supported consistent abundances of *E. coli* as ancestral NifA*-based cocultures, a trait
318 which we know is dependent on the level of NH_4^+ excretion (17-19). Our results
319 therefore suggest that the NifA* mutation, a 48 bp deletion, is not prone to frequent
320 suppression, potentially because multiple mutations would be required. Based on our
321 findings, we propose that experimental evolution is a valuable approach both for
322 identifying novel genotypes enabling coexistence within synthetic consortia and for
323 assessing the long-term stability of putatively costly engineered genotypes.

324 More broadly, our results indicate that within a cross-feeding partnership, multiple
325 combinations of recipient and producer genotypes can lead to stable coexistence but
326 only certain combinations will be favored to evolve based on the selective environment.
327 Under well-mixed conditions, like those in most of our experiments here, there is intense
328 competition between recipients as well as producers for limiting, communally-valuable
329 nutrients, such as NH_4^+ (18), vitamins, or amino acids (1, 7, 8). Additionally, there is a
330 probable fitness cost for producers associated with increased nutrient excretion in well-
331 mixed environments. Under well-mixed conditions, costless self-serving and mutually
332 beneficial mutations, but not costly partner-serving mutations, are favored to evolve
333 (34). Therefore mutations that improve a recipient's ability to acquire key nutrients from
334 producers, and thereby outcompete other recipient genotypes, can evolve rapidly (35).
335 These recipient mutations that enhance metabolite uptake also erode the partial
336 privatization of communally valuable nutrients released by the producer (36). Even so,
337 these recipient mutations can benefit producers if they promote mutualistic interactions
338 (35). We view the *E. coli* $NtrC^{S163R}$ mutation as an example of costless self-serving
339 mutation, given its rapid emergence in well-mixed cocultures, but one that is mutually

beneficial as an obligate mutualism results. However, we hypothesize that the benefits of the NtrC^{S163R} mutation extend more generally to surviving nitrogen limitation. In support of this, it was shown that an NtrC^{V18L} mutation that similarly increased *amtB* expression was adaptive for *E. coli* evolved in nitrogen-limiting monocultures (37). The general benefit in surviving nitrogen limitation might also explain why *E. coli* NtrBC mutations were also observed in evolved static cocultures (Table S1), where cells settle into dense populations at the bottom of the test tube that likely intensify competition for NH_4^+.

Mutations that improve nutrient acquisition can be mutually beneficial for cross-feeding partners under conditions such as those used in our study, where neither species can grow well without reciprocal nutrient exchange. However, mutations that enhance nutrient uptake could also be adaptive for the recipient when there is no reciprocal benefit to the producer. Consequently, mutations that enhance nutrient uptake could result in the emergence of mutualistic, commensal, or competitive interactions, depending on the microbial community composition and conditions (35). In natural microbial communities, where auxotrophy is prevalent (1, 7) and most cells exhibit low metabolic activity, including dormant or growth-arrested states (9, 10), mutations that improve acquisition of limiting nutrients, could allow certain populations to flourish. Understanding the consequences of mutations that expedite metabolite acquisition could thus inform on the origins of microbial mutualisms and the mechanisms that underpin other ecological relationships. This knowledge could ultimately be harnessed for various applications, ranging from facilitating coexistence within synthetic consortia to probiotic-mediated competitive exclusion of pathogens.

Methods.

Strains and growth conditions. All strains and plasmids are listed in SI Appendix Table S2. *E. coli* was grown in Luria-Bertani (LB) Miller broth or on LB agar at 30 or 37°C supplemented with gentamicin (Gm; 5-15 µg/ml), kanamycin (Km; 30 µg/ml), or carbenicillin (100 µg/ml) when appropriate. *R. palustris* was grown in defined minimal photosynthetic medium (PM) (38) or on PM agar with 10 mM succinate at 30°C and supplemented with gentamycin (100 µg/ml) when appropriate. N_2-fixing medium (NFM) was made by omitting $(NH_4)_2SO_4$ from PM. NFM and LB agar were used as selective media to quantify *R. palustris* and *E. coli* CFUs, respectively. Monocultures were grown in 10 ml of M9-derived coculture medium (MDC) and cocultures in 10 ml of MDC in 27 ml anaerobic test tubes. Tubes were made anaerobic under 100% N_2, sterilized, and supplemented with 1 mM $MgSO_4$ and 0.1 mM $CaCl_2$ as described (17). *E. coli* starter monocultures had 25 mM glucose and were growth-limited by supplementing with 1.5 mM NH_4Cl. *R. palustris* starter monocultures were growth-limited by supplementing with limiting 3 mM acetate. Cocultures were inoculated by subculturing 1% v/v of starter monocultures of each species into MDC with 50 mM glucose. Mono- and cocultures were grown at 30°C, under well-mixed conditions, lying horizontally and shaking at 150 rpm beneath a 60 W incandescent bulb or, where indicated, under static conditions, standing vertically and not shaken during growth beside a 60 W incandescent bulb.

Construction of *E. coli* NtrC^{S163R}. All primers are listed in Table S3. The Gm^R-*sacB* genes from pJQ200SK (39) were PCR amplified using primers containing ~40 bp overhanging regions with homology up and downstream of *ntrC* (*glnG*). A second round of PCR was then performed to increase the length of overhanging regions to ~80 bp

386 and thereby increase recombination frequency. *E. coli* MG1655 harboring pKD46
387 encoding arabinose-inducible λ-red recombineering genes (40) was grown in LB with
388 carbenicillin and 20 mM arabinose at 30°C to an OD_{600} of ~0.5 and then centrifuged,
389 washed, and resuspended in sterile distilled water at ambient temperature.
390 Resuspended *E. coli* cells were electroporated with Gm^R-*sacB* PCR product with ~80 bp
391 of homology flanking *ntrC*. Gm-resistant colonies were screened by PCR and site-
392 directed recombination of Gm^R-*sacB* into the *ntrC* locus, creating a Δ*ntrC*::Gm^R-*sacB*
393 allele, was verified by sequencing. To replace the ΔntrC::Gm^R-*sacB* locus, the $NtrC^{S163R}$
394 allele was PCR-amplified from gDNA of evolved *E. coli* (lineage A25) and
395 electroporated into *E. coli* ΔNtrC::Gm^R-*sacB* harboring pKD46. After counterselection on
396 LB agar without NaCl and supplemented with 10% (w/v) sucrose, site-directed
397 recombination of the $NtrC^{S163R}$ allele into the native locus was confirmed by PCR and
398 sequencing. *E. coli* $NtrC^{S163R}$ was grown overnight on LB agar at 42°C to cure the strain
399 of pKD46. Loss of pKD46 was confirmed by lack of growth with carbenicillin.

400 ***R. palustris* strain construction**. The WT and NifA* *R. palustris* strains used for
401 experiments in Fig. 1 were the type strain CGA009 (38) and CGA676, respectively.
402 CGA676 carries a 48 bp deletion in *nifA* (24). The *R. palustris* strains used in
403 experimental coculture evolution and subsequent experiments were CGA4001 and
404 CGA4003, which are derived from CGA009 and CGA676, respectively, with both
405 carrying an additional Δ*hupS* mutation, preventing the oxidation of H_2. To construct *R.*
406 *palustris* CGA4001 and CGA4003, pJQ-Δ*hupS* was introduced into *R. palustris*
407 CGA009 and CGA676, respectively, by conjugation with *E. coli* S17-1. Mutants were

then obtained using sequential selection and screening as described (41). The Δ*hupS* deletion was confirmed by PCR and sequencing.

Analytical procedures. Cell densities were approximated by optical density at 660 nm (OD_{660}) using a Genesys 20 visible spectrophotometer (Thermo-Fisher). Coculture doubling times were derived from specific growth rates determined by fitting exponential functions to OD_{660} measurements between 0.1-1.0 for each biological replicate. NH_4^+ was quantified using an indophenol colorimetric assay (17). Glucose and soluble fermentation products were quantified using a high-performance liquid chromatograph (Shimadzu) as described (42). H_2 was quantified using a gas chromatograph (Shimadzu) with a thermal conductivity detector as described (43).

Coculture evolution experiments. Founder monocultures of *E. coli* MG1655, *R. palustris* CGA4001 (Δ*hupS*), and CGA4003 (Δ*hupS* NifA*) were inoculated from single colonies in MDC. Once grown, a single founder monoculture of each strain was used to inoculate twelve WT-based cocultures (six well-mixed: A-F; six static: G-L) and 12 NifA*-based cocultures (six well-mixed: M-R; six static: S-X) in MDC with 50 mM glucose. Cocultures were serially transferred by passaging 2% v/v of stationary phase coculture (OD_{660} > 2) into fresh MDC. The NifA*-based cocultures were transferred weekly whereas WT-based cocultures were transferred every 30-50 days for the first five transfers and then every two-weeks after that. For comparative analyses, well-mixed cocultures (A-F and M-R) were revived from frozen stocks made following serial transfer 2 (generation 17) and transfer 25 (generation 146) by thawing ~0.2 ml of coculture in 1 ml sterile MDC. Thawed cocultures were washed 2X with MDC to remove

glycerol from frozen stocks and then resuspended in 0.2 ml MDC before inoculating into MDC with 50 mM glucose.

RNA extraction and reverse transcription quantitative PCR. RNA was isolated from exponentially growing *E. coli* monocultures or starved cell suspensions that had been chilled on ice, centrifuged at 4°C, and the resulting cell pellets flash frozen using dry-ice in ethanol and stored at -80°C. Cell pellets were thawed on ice, disrupted by bead beating, and then RNA was purified using an RNeasy MiniKit (Qiagen), Turbo DNase (Ambion) treatment on columns, and RNeasy MinElute Cleanup Kit (Qiagen). The cDNA was synthesized from 0.5-1 µg of RNA per sample using Protoscript II RT and Random Primer Mix (New England Biolabs). The qPCR reactions were performed on cDNA samples using iQ SYBR Green supermix (BioRad). *E. coli* genomic DNA was used to generate standard curves for *amtB* and *ntrC* transcript quantification, which were normalized to transcript levels of reference/housekeeping genes *gyrB* and *hcaT* (44). Duplicate technical replicate qPCR reactions were performed and averaged for each biological replicate to calculate relative expression.

Genome sequencing and mutation analysis. Genomic DNA was extracted from stationary phase evolved cocultures following revival from frozen stocks using a Wizard® Genomic DNA purification Kit (Promega). DNA fragment libraries were constructed for samples from evolved shaking WT-based cocultures A25, B24-F24 and NifA*-based cocultures M30-R30 using NextFlex Bioo Rapid DNA kit. Samples were sequenced on an Illumina NextSeq 500 150 bp paired-end run by the Center for Genomics and Bioinformatics at Indiana University, Bloomington. After trimming paired-end reads using Trimmomatic 0.36 (45) with the following options: LEADING:3

453 TRAILING:3 SLIDINGWINDOW:10:26 HEADCROP:10 MINLEN:36. Mutations were
454 called using *breseq* version 0.32.0 on Polymorphism Mode (46) and compared to a
455 reference genome created by concatenating *E. coli* MG1655 (Accession NC_000913),
456 *R. palustris* CGA009 (Accession BX571963), and its plasmid pRPA (Accession
457 BX571964). Mutations are summarized in Supplemental File 1.

458 Additional gDNA sequencing for evolved WT-based cocultures A1-F1 (shaking), G1-L1
459 (static), G21-L21 (static), and NifA*-based cocultures S21-X21 (static) was performed at
460 the Department of Energy Joint Genome Institute. Plate-based DNA library preparation
461 for Illumina sequencing was performed on the PerkinElmer Sciclone NGS robotic liquid
462 handling system using Kapa Biosystems library preparation kit. 200 ng of gDNA was
463 sheared using a Covaris LE220 focused-ultrasonicator. Sheared DNA fragments were
464 size selected by double-SPRI and then the selected fragments were end-repaired, A-
465 tailed, and ligated with Illumina compatible sequencing adaptors from IDT containing a
466 unique molecular index barcode for each sample library. Libraries were quantified using
467 KAPA Biosystem's next-generation sequencing library qPCR kit and run on a Roche
468 LightCycler 480 real-time PCR instrument. The quantified libraries were then prepared
469 for sequencing on the Illumina HiSeq sequencing platform utilizing a TruSeq Rapid
470 paired-end cluster kit. Sequencing of the flowcell was performed on the Illumina
471 HiSeq2500 sequencer using HiSeq TruSeq SBS sequencing kits, following a 2x100
472 indexed run recipe. Reads were aligned to a reference genome created by
473 concatenating *E. coli* MG1655 (Accession NC_000913), *R. palustris* CGA009
474 (Accession NC_005296), and its plasmid pRPA (Accession NC_005297) (47). The
475 resulting bams were then split by organism and down sampled to 100 fold depth if in

476 excess of that, then re-merged to create a normalized bam for calling single nucleotide
477 polymorphisms and small indels by callVariants.sh from the BBMap package
478 (sourceforge.net/projects/bbmap/) to capture variants present within the population and
479 annotation applied with snpEff (48). Mutations are summarized in Supplemental File 2.

480 All FASTQ files are available at NCBI Sequence Read Archive (Accession numbers
481 listed in Table S1)

482 **Acknowledgements**

483 This work was supported in part by U.S. Army Research Office grants W911NF-14-1-
484 0411 and W911NF-17-1-0159, a National Science Foundation CAREER award, grant
485 MCB-1749489, and the U.S. Department of Energy, Office of Science, Office of
486 Biological and Environmental Research, under award number DE-SC0008131 and the
487 Joint Genome Institute Community Science Program, CSP 502893. The work
488 conducted by the U.S. Department of Energy Joint Genome Institute, a DOE Office of
489 Science User Facility, is supported by the Office of Science of the U.S. Department of
490 Energy under Contract No. DE-AC02-05CH11231.

491 We are grateful to AL Posto, JR Gliessman, and MC Onyeziri for assistance with
492 passaging and initial coculture characterization, to JT Lennon and BK Lehmkuhl for use
493 of equipment and assistance with qPCR experiments, and to J Ford and AM Buechlein
494 at the IU Center for Genomics and Bioinformatics.

495 **Author contributions.** RKF and JBM designed the experiments. JTB, MGB, AL, and
496 JM performed the bioinformatics analyses. RKF performed all wet lab experiments and

497 analyzed the data. RKF wrote the first manuscript draft. RKF and JBM edited the

498 manuscript. All authors read and approved the final manuscript draft.

499

Figures and legends

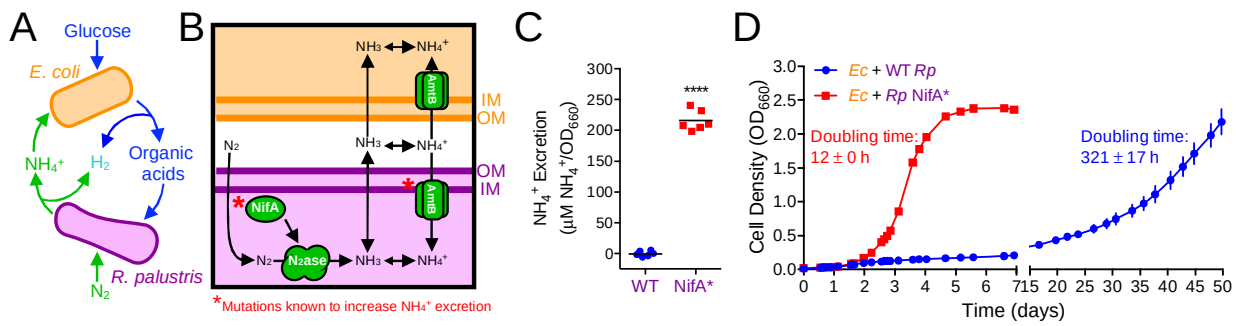

Fig. 1. Mutualistic cross-feeding between *E. coli* and *R. palustris* is facilitated by NH_4^+ excretion. (A) Coculture growth requires reciprocal cross-feeding of organic acids and NH_4^+ excreted by *E. coli* and *R. palustris*, respectively. (B) Mechanism of NH_4^+ cross-feeding from *R. palustris* to *E. coli* and mutational targets known to increase NH_4^+ excretion by *R. palustris* (*). (C) NH_4^+ excretion levels by WT *R. palustris* (CGA009) and an isogenic NifA* mutant (CGA676) in carbon-limited N_2-fixing monocultures grown in grown in MDC or NFM minimal medium, with similar results observed for both media. Points are biological replicates and lines are means, n=6; paired t-test, ****p<0.0001. (D) Coculture growth curves (both species) of *E. coli* paired with either WT *R. palustris* or the NifA* mutant. Points are means ± SEM, n=3. Doubling times are means ± SD.

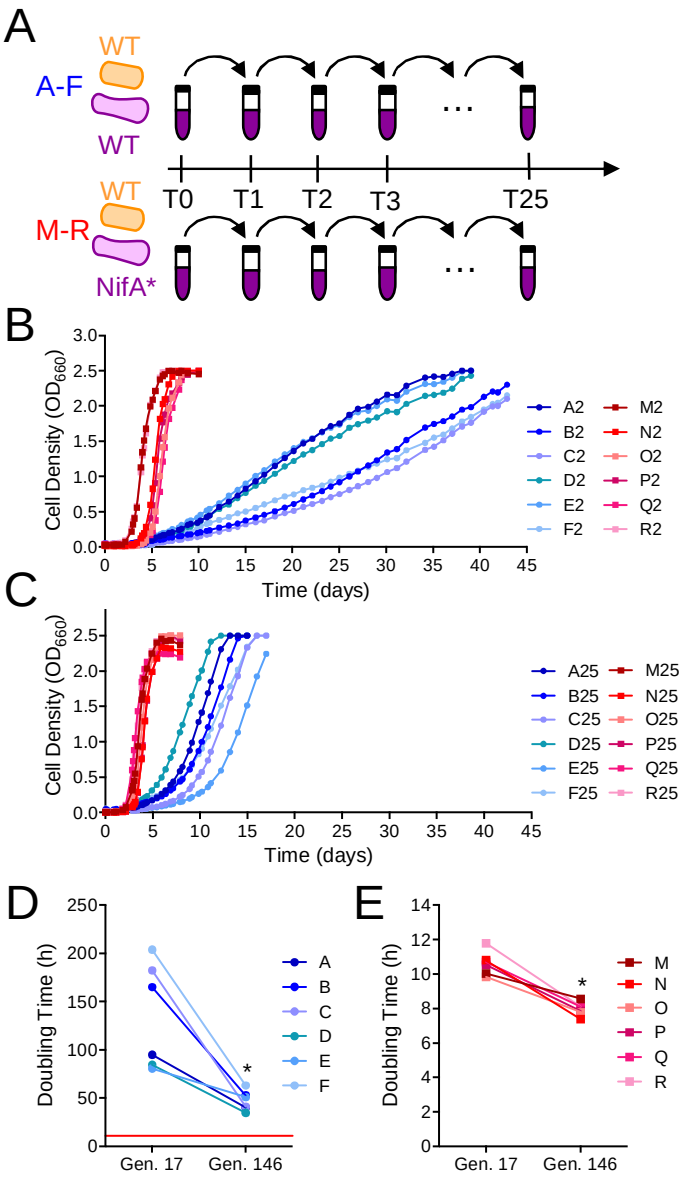

Fig. 2. Coculture doubling times decreased during experimental evolution of WT-based (CGA4001; blue) and NifA*-based (CGA4003; red) cocultures. Points are values for the indicated individual revived coculture lineages. (A) Design for experimental evolution of parallel WT-based (A-F) and NifA*-based (M-R) cocultures via serial transfer. (B, C) Growth curves (both species) of WT-based (blue circles) and NifA*-based (red squares) cocultures revived after two transfers (17 generations) (B) or 25 transfers (146 generations) (C) of experimental evolution. Different shades indicate the different lineages. (D, E) Coculture doubling times (both species) of individual WT-based cocultures (D) or NifA* based cocultures (E) at generation (Gen.) 17 and 146 (*, Wilcoxon matched-pairs signed rank, p=0.0313). (D) The red line indicates the doubling time of NifA*-based cocultures at Gen. 17.

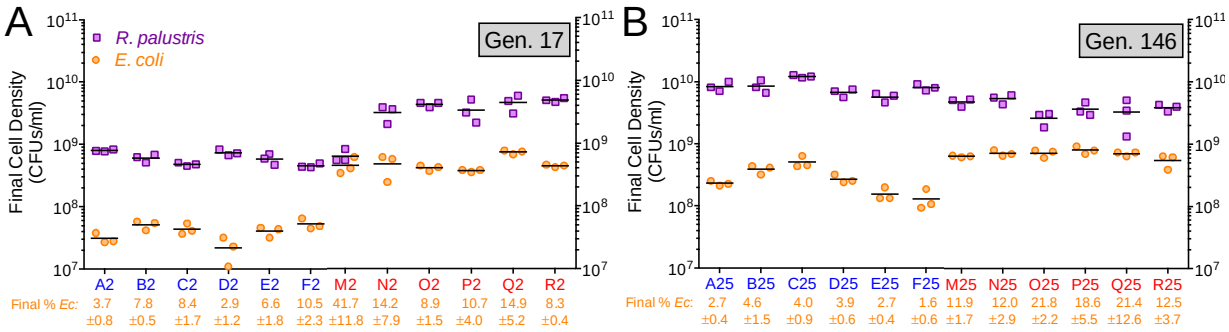

Fig. 3. Final cell densities for each species increase in WT-based cocultures between generation 17 (A) and generation 146 (B). (A, B) Final viable cell densities of *R. palustris* and *E. coli* and the final *E. coli* percentage (± SD) for WT-based (CGA4001; blue) and NifA*-based (CGA4003; red) cocultures at the final time points shown in Fig 2B and 2C. Points represent biological replicates and lines are means, n=3. Triplicate technical replicate plating was performed for each biological replicate. The lower *R. palustris* CFUs in the M2 coculture was due to plate contamination that obscured accurate CFU enumeration. The average final *E. coli* percentage in NifA*-based cocultures did not significantly differ whether we included or excluded M2 values (Wilcoxon matched-pairs signed rank test, P=0.563 or 0.125).

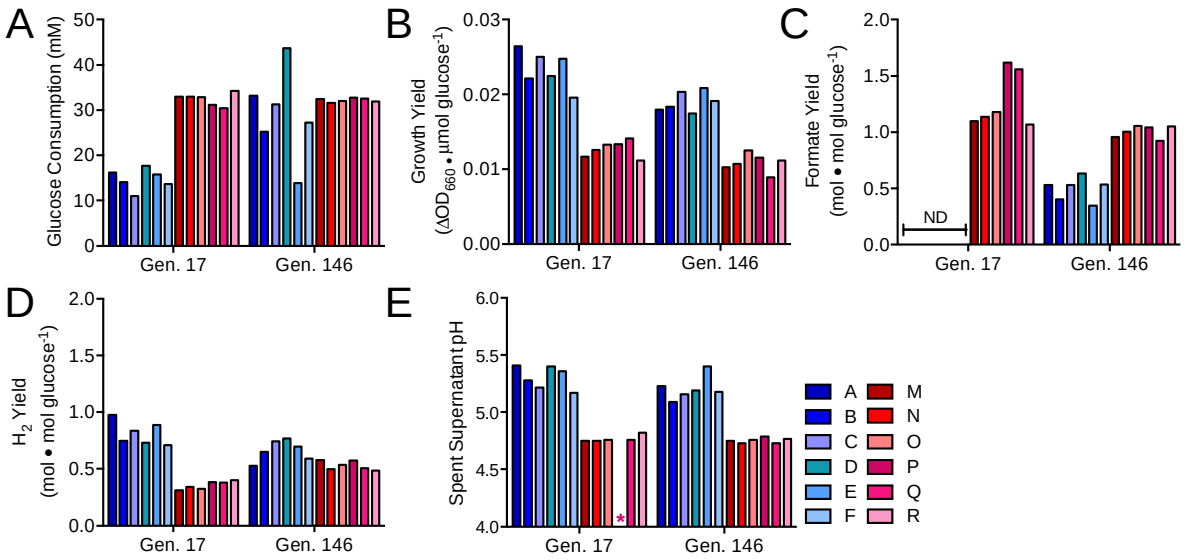

536

537

538 **Fig. 4.** WT-based (blue) and NifA*-based (red) cocultures exhibit distinct metabolic
539 phenotypes. Bars are individual values for glucose consumption (A), growth yield (B),
540 formate yield (C), H_2 yield (D), and final pH (E) for the indicated WT-based (CGA4001;
541 blue) and NifA*-based (CGA4003; red) revived coculture lineages at generation (Gen)
542 17 and 146. Different shades indicate different lineages. ND, not detected. Asterisk (*)
543 indicates that the pH for lineage P at G17 was not quantified because culture tube broke
544 prior to measurements.

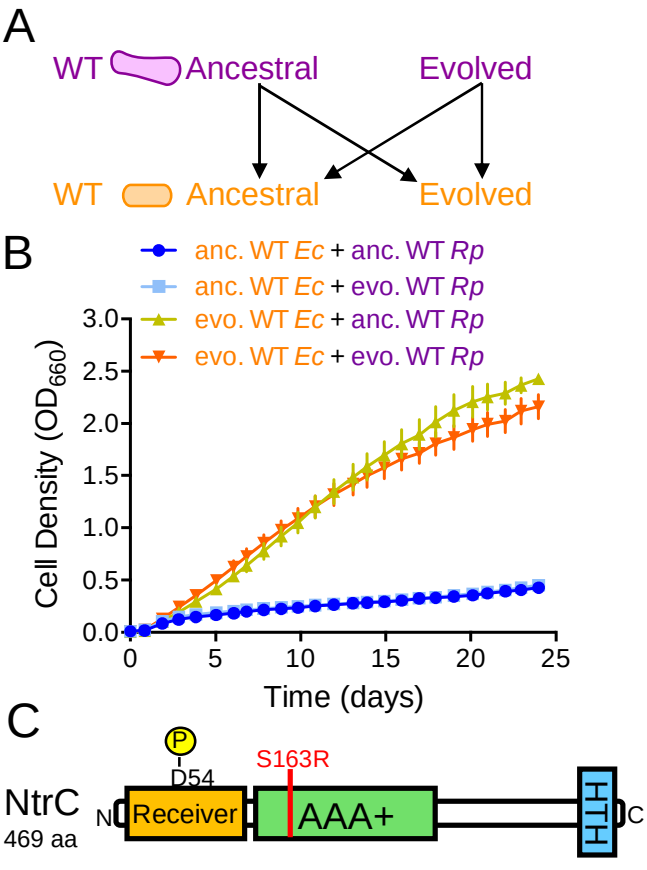

Fig. 5. Adaptation by *E. coli* is sufficient to enable growth of WT-based cocultures. Ancestral (anc) and evolved (evo) WT *R. palustris* (CGA4001) and WT *E. coli* were paired in all possible combinations (A) and the growth of the cocultures (both species) was monitored (B). (B) Points are means ± SEM, n=3. (C) The location (red line) of the missense mutation in *E. coli* NtrC, which was fixed in all six parallel evolved *E. coli* populations from WT-based cocultures at G140-146.

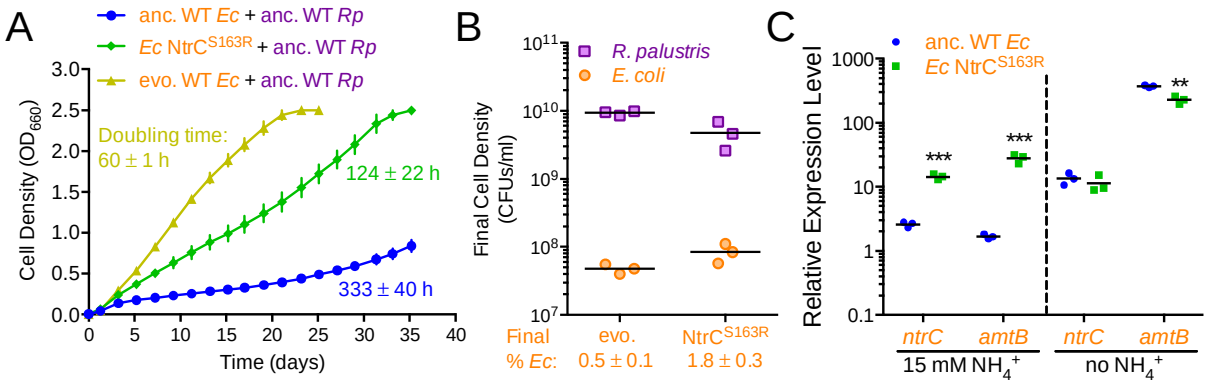

553

554 **Fig. 6.** A missense mutation in *E. coli ntrC* enables emergent NH_4^+ cross-feeding by
555 conferring constitutive expression of nitrogen acquisition. (A) Coculture growth curves
556 (both species) of ancestral (anc) WT, evolved (evo) WT, and the $NtrC^{S163}$ mutant *E. coli*
557 paired with ancestral WT *R. palustris* (CGA4001). Points are means ± SEM, n=3. Mean
558 doubling times (± SD) are listed next to each growth curve. (B) Final cell densities of
559 each species and *E. coli* frequencies in cocultures with evolved WT *E. coli* and the
560 $NtrC^{S163}$ mutant at the final time points shown in panel A. Triplicate technical replicate
561 plating was performed for each biological replicate. Final *E. coli* frequencies are the
562 mean ± SD. (C) Relative expression of *ntrC* and *amtB* genes in ancestral WT *E. coli* and
563 the $NtrC^{S163}$ mutant when grown in monoculture with 15 mM NH_4Cl or under complete
564 NH_4Cl starvation. (B, C) Points represent biological replicates and lines are means, n=3;
565 Holm-Sidak t-test, $^{**}p<0.01$, $^{***}p<0.001$). RT-qPCR experiments were performed with
566 duplicate technical replicates for each biological replicate. *E. coli hcaT* was used for
567 normalization. Similar results were observed with *gyrB* and with multiple primer sets for
568 both the target and reference housekeeping genes.

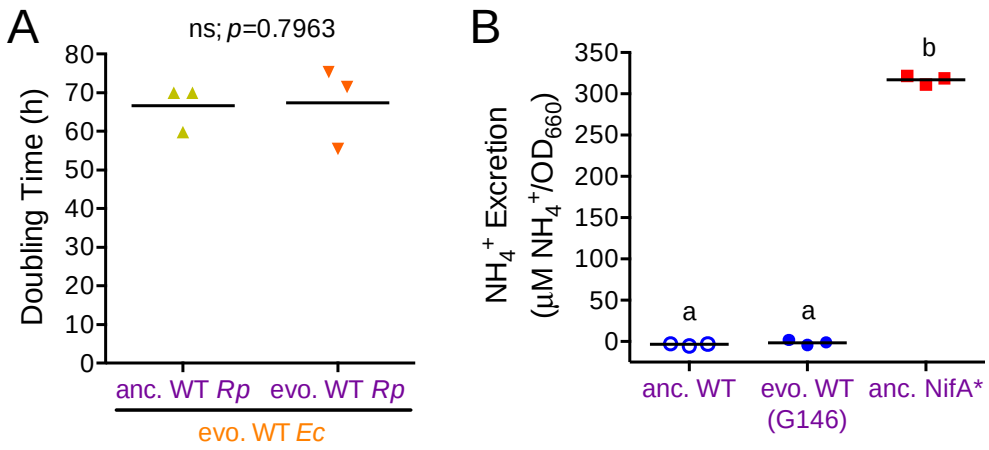

Fig. S1. Evolution of WT *R. palustris* in coculture with *E. coli* does not affect coculture doubling times nor NH_4^+ excretion levels. (A) Coculture doubling time of evolved WT *E. coli* (G146, A25 isolates) paired with ancestral or evolved WT *R. palustris* (CGA4001; G146, A25 isolates). Points represent biological replicates and lines are means, n=3; paired t-test, p=0.7963; ns, not significant). (B) NH_4^+ excretion by ancestral and evolved WT *R. palustris* and the NifA* mutant during carbon-limited N_2-fixing monoculture growth. Points represent biological replicates and lines are means, n=3; One-way ANOVA with Tukey's multiple comparisons test, different letters indicate significant statistical differences, p<0.0001).

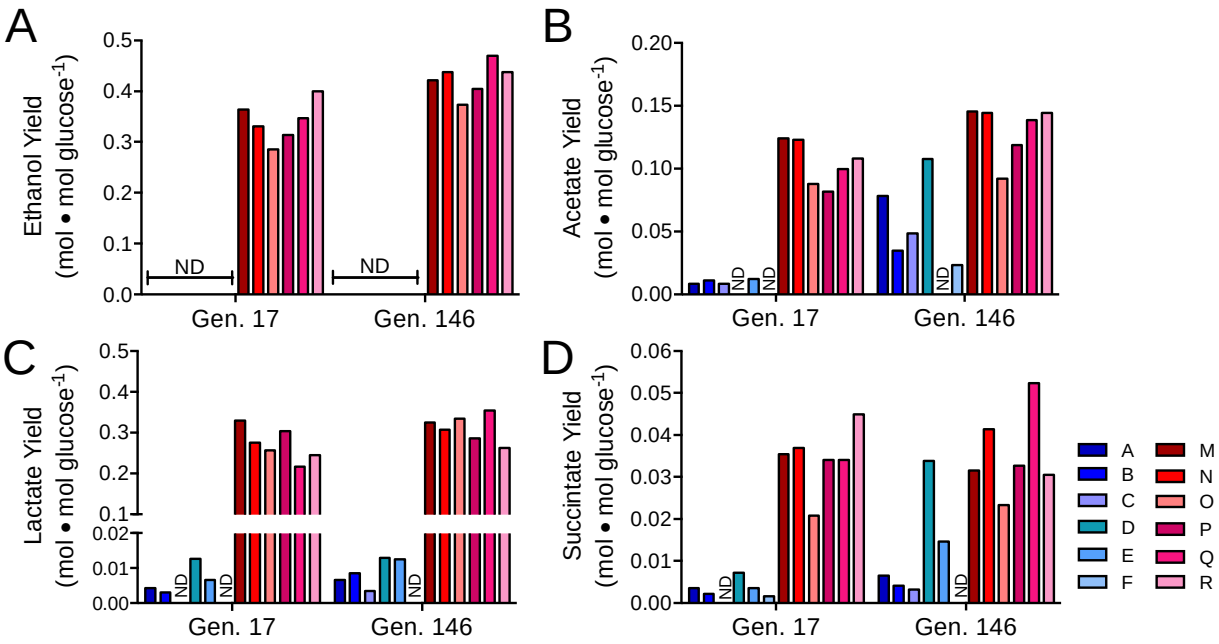

579

580 **Fig. S2.** Other evolved coculture fermentation product yields also differ between WT-
581 based and NifA*-based cocultures. Bars are individual yields for ethanol (A), acetate
582 (B), lactate (C), and succinate (D), for the indicated WT-based (CGA4001; blue) and
583 NifA*-based (CGA4003; red) revived coculture lineages at generation (Gen) 11 and
584 146. Different shades indicate different lineages. ND, not detected.

585 **Table S1. Mutations in *ntrBC* genes in *E. coli* following coculture evolution**

Lineage	Gene	Mutation	Generation	Frequency	*R. palustris* partner strain	Growth condition	SRA Accession
A	*ntrC*	S163R	11	100%	WT	Mixed	SRX5772396
A	*ntrC*	S163R	146	100%	WT	Mixed	SRX5872514
B	*ntrC*	S163R	11	NC[a]	WT	Mixed	SRX5772395
B	*ntrC*	S163R	140	100%	WT	Mixed	SRX5872520
C	*ntrC*	S163R	11	NC[a]	WT	Mixed	SRX5772261
C	*ntrC*	S163R	140	100%	WT	Mixed	SRX5874533
D	*ntrC*	S163R	11	NC[a]	WT	Mixed	SRX5772258
D	*ntrC*	S163R	140	100%	WT	Mixed	SRX5874537
E	*ntrC*	S163R	11	NC[a]	WT	Mixed	SRX5772266
E	*ntrC*	S163R	140	100%	WT	Mixed	SRX5874556
F	*ntrC*	S163R	11	NC[a]	WT	Mixed	SRX5209606
F	*ntrC*	S163R	140	100%	WT	Mixed	SRX5874560
G	*ntrC*	S163R	11	NC[a]	WT	Static	SRX5772260
G	*ntrC*	S163R	123	100%	WT	Static	SRX5772001
H	*ntrC*	S163R	11	63%	WT	Static	SRX5772264
H	*ntrC*	S163R	123	76%	WT	Static	SRX5771991
I	*ntrC*	S163R	11	NC[a]	WT	Static	SRX5772259
I	*ntrC*	S163R	123	100%	WT	Static	SRX5771995
J	*ntrB*	R116S	11	NC[a]	WT	Static	SRX5772262
J	*ntrB*	R116S	123	100%	WT	Static	SRX5771992
K	*ntrC*	S163R	11	80%	WT	Static	SRX5772263
K	*ntrC*	S163R	123	100%	WT	Static	SRX5771996
L	*ntrC*	S163	11	NC[a]	WT	Static	SRX5772265
M	*ntrC*	H184Y	174	79%	NifA*	Mixed	SRX5874674
N	*ntrB*	A175V	174	39%	NifA*	Mixed	SRX5875647
N	*ntrC*	D109V	174	10%	NifA*	Mixed	SRX5875647
N	*ntrC*	G373V	174	44%	NifA*	Mixed	SRX5875647
O	*ntrB*	P336Q	174	41%	NifA*	Mixed	SRX5877494
O	*ntrC*	Q374H	174	54%	NifA*	Mixed	SRX5877494
P	*ntrB*	R116H	174	32%	NifA*	Mixed	SRX5877497
Q	ND[b]	-	-	-	NifA*	Mixed	SRX5910505
R	ND[b]	-	-	-	NifA*	Mixed	SRX5910551
S	*ntrB*	L137V	123	23%	NifA*	Static	SRX5771990
S	*ntrC*	S45R	123	7%	NifA*	Static	SRX5771990
T	*ntrB*	G150C	123	15%	NifA*	Static	SRX5771989
U	*ntrB*	A175V	123	65%	NifA*	Static	SRX5771988
V	ND[b]	-	-	-	NifA*	Static	SRX5771994
W	ND[b]	-	-	-	NifA*	Static	SRX5771993

X	*ntrB*	A175V	123	13%	NifA*	Static	SRX5771967
X	*ntrB*	V305F	123	16%	NifA*	Static	SRX5771967
X	*ntrC*	E116K	123	17%	NifA*	Static	SRX5771967

[a]Frequency was not calculated (NC) because read coverage <10.

[b]*ntrBC* mutations were not detected (ND) in population. Mutations present at frequencies <1% are not listed.

Table S2. Strains and plasmids

Strain or plasmid	Genotype (text designation); Phenotype/description	Reference, origin, or description
R. palustris strains		
CGA009	Wild-type strain (14); spontaneous Cm^R derivative of CGA001	(49)
CGA676	NifA* (NifA*); derivative of CGA009 with 48 bp deletion of NifA Q-linker (amino acids 202-217) conferring constitutive nitrogenase expression	(24)
CGA4001	Δ*hupS* (anc. WT); Ancestral strain for experimentally evolved WT-based cocultures A-F; derivative of CGA009 with inactive uptake hydrogenase	This study
CGA4003	*nifA** Δ*hupS* (anc.NifA*); Ancestral strain for experimentally evolved NifA*-based cocultures M-R; derivative of CGA009 with constitutive nitrogenase expression and inactive uptake hydrogenase	This study
E. coli strains		
MG1655	Wild-type K-12 strain (WT/anc.); ancestral *E. coli* strain for all experimental evolution lineages	(50)
MG1655 $NtrC^{S163R}$	$NtrC^{S163R}$ ($NtrC^{S163R}$); MG1655 derivative with serine 163 to arginine (S163R) point mutation of NtrC	This study
S17-1	*thi pro hdsR hdsM*$^+$ *recA*; chromosomal insertion of RP4-2 (Tc::Mu Km::Tn7);	(51)
Plasmids		
pJQ200SK	Gm^R, *sacB*; mobilizable suicide vector	(39)
pJQ-ΔhupS	pJQ200SK with DNA fragments flanking *hupS* fused by PCR to generate unmarked, in-frame deletion of *hupS* in *R. palustris*	(17)
pKD46	Cb^R; temperature-sensitive plasmid with arabinose-inducible λ-Red recombination system for recombineering of *E. coli*	(40)

592 **Table S3. Primers**

Primer	Sequence (5'→3'); Restriction site	Purpose
Cloning primers		
sacB-Gm^R Fwd	CAGCAATTTGCGCTCAATAATCAATCTTTACACACAAGCT GTGAAGCTAGAGGATCGATCCTTTTTAACC	Amplifying *sacB*-GmR from pJQ200SK with 45 bp *ntrC* upstream flanking region
sacB-Gm^R Rev	CGAGTTCTCGGTTTACCTGCCTATCAGGAAATAAAGGTG ACGTTTGAAACGGATGAAGGCACGAAC	Amplifying *sacB*-GmR from pJQ200SK with 45 bp *ntrC* downstream flanking region
ntrC us R2	CATACTGAACTTATCGGAACAGTAAAGCGTAAAATACCA GCAATTTGCGCTCAATAATC	Adding additional 35 bp of *ntrC* upstream flanking region to sacB-GmR product in 2nd round of PCR for λ-Red recombineering
ntrC ds R2	CAGGCAAAATTGAATTTACCAGTTGGCCAGGGCATACCG AGTTCTCGGTTTACCTGC	Adding additional 35 bp of ntrC downstream flanking region to sacB-GmR product in 2nd round of PCR for λ-Red recombineering
ntrC Fwd	GCGCGGATTGATGTGGAAG	Amplfying *E. coli* ntrC with >200 bp upstream stream flanking region from evolved *E. coli* for λ-Red recombineering
ntrC Rev	CAGCTAAACAGCCCAATCATTG	Amplfying *E. coli* ntrC with ~200 bp downstream flanking region from evolved *E. coli* for λ-Red recombineering
ALP011	TGGATCCGCGACACCTCGCTGTCG	Amplifying *R. palustris hupS* upstream flanking region for in-frame deletion; BamHI
ALP012	CCGTTGGAGGTGCCGGGTACCCTCGTAAAAGGTTTCCG TCACTGC	Amplifying *R. palustris hupS* upstream flanking region for in-frame deletion
ALP013	GAAACCTTTTACGAGGGTACCCGGCACCTCCAACGGCA AGTCGGC	Amplifying *R. palustris hupS* downstream flanking region
ALP014	TTCTAGAACCCGGCAATCGCCACC	Amplifying *R. palustris hupS* downstream flanking region; XbaI
qPCR primers		
qPCR *amtB* Fwd1	GGATGATCCCTGCGATGTCTT	Quantifying *E. coli*

		amtB expression from cDNA; set 1
qPCR *amtB* Rev1	CGAGCTGGCGGCAAAAATC	Quantifying *E. coli amtB* expression from cDNA; set 1
qPCR *amtB* Fwd2	GCGGTGATGGGCAGCATTTATC	Quantifying *E. coli amtB* expression from cDNA; set 2
qPCR amtB Rev2	AGCGCCCCAACTATCAAGC	Quantifying *E. coli amtB* expression from cDNA; set 2
qPCR *ntrC* Fwd1	GGAATAATGTACCGCCATCGGC	Quantifying *E. coli ntrC* expression from cDNA; set 1
qPCR *ntrC* Rev1	ATCAGAACTGTTTGGCCACGAG	Quantifying *E. coli ntrC* expression from cDNA; set 1
qPCR *ntrC* Fwd2	ACTCTCCGCAACCGTTGATTC	Quantifying *E. coli ntrC* expression from cDNA; set 2
qPCR NtrC Rev2	AGCTGGAAAACACCTGCCG	Quantifying *E. coli ntrC* expression from cDNA; set 2
qPCR hcaT Fwd	CGTGGTGGCGGAAGTCATTATC	Quantifying *E. coli hcaT* expression from cDNA; housekeeping reference gene
qPCR hcaT Rev	CGCCGAGATCAACAGCATATCG	Quantifying *E. coli hcaT* expression from cDNA; housekeeping reference gene
qPCR gyrB Fwd	CGTAGATCTGACGGTGAATTT	Quantifying *E. coli gyrB* expression from cDNA; housekeeping reference gene
qPCR gyrB Rev	CGTTGGTGTTTCGGTAGTA	Quantifying *E. coli gyrB* expression from cDNA; housekeeping reference gene

Supplemental File 1. Mutations identified in evolved WT-based cocultures A25, B24-F24 and NifA*-based cocultures M30-R30 using *breseq*.

Supplemental File 2. Mutations identified in evolved WT-based cocultures A1-F1 (shaking), G1-L1 (static), G21-L21 (static), and NifA*-based cocultures S21-X21 (static) using the BBMap package

References

1. E. C. Seth, M. E. Taga, Nutrient cross-feeding in the microbial world. *Front. Microbiol.* **5** (2014).
2. S. Estrela, C. H. Trisos, S. P. Brown, R. Associate Editor: Pejman, D. Editor: Troy, From Metabolism to Ecology: Cross-Feeding Interactions Shape the Balance between Polymicrobial Conflict and Mutualism. *Am. Nat.* **180**, 566-576 (2012).
3. B. E. L. Morris, R. Henneberger, H. Huber, C. Moissl-Eichinger, Microbial syntrophy: interaction for the common good. *FEMS Microbiol. Rev.* **37**, 384-406 (2013).
4. O. Ponomarova, K. R. Patil, Metabolic interactions in microbial communities: untangling the Gordian knot. *Curr. Opin. Microbiol.* **27**, 37-44 (2015).
5. A. Zelezniak *et al.*, Metabolic dependencies drive species co-occurrence in diverse microbial communities. *Proc. Natl. Acad. Sci. U S A* **112**, 6449-6454 (2015).
6. M. Embree, J. K. Liu, M. M. Al-Bassam, K. Zengler, Networks of energetic and metabolic interactions define dynamics in microbial communities. *Proc. Natl. Acad. Sci. U S A* **112**, 15450-15455 (2015).
7. K. Zengler, L. S. Zaramela, The social network of microorganisms — how auxotrophies shape complex communities. *Nat. Rev. Microbiol.* **16**, 383-390 (2018).
8. M. T. Mee, J. J. Collins, G. M. Church, H. H. Wang, Syntrophic exchange in synthetic microbial communities. *Proc. Natl. Acad. Sci. U S A* **111**, E2149-E2156 (2014).
9. M. Bergkessel, D. W. Basta, D. K. Newman, The physiology of growth arrest: uniting molecular and environmental microbiology. *Nat. Rev. Microbiol.* **14**, 549 (2016).
10. J. T. Lennon, S. E. Jones, Microbial seed banks: the ecological and evolutionary implications of dormancy. *Nat. Rev. Microbiol.* **9**, 119 (2011).
11. B. Momeni, C.-C. Chen, K. L. Hillesland, A. Waite, W. Shou, Using artificial systems to explore the ecology and evolution of symbioses. *Cell. Molec. Life Sci.* **68**, 1353 (2011).
12. M. T. Mee, H. H. Wang, Engineering ecosystems and synthetic ecologies. *Mol. Biosyst.* **8**, 2470-2483 (2012).
13. S. R. Lindemann *et al.*, Engineering microbial consortia for controllable outputs. *ISME J.* **10**, 2077 (2016).
14. S. Widder *et al.*, Challenges in microbial ecology: building predictive understanding of community function and dynamics. *ISME J.* **10**, 2557 (2016).
15. K. L. Hillesland, D. A. Stahl, Rapid evolution of stability and productivity at the origin of a microbial mutualism. *Proc. Natl. Acad. Sci. U S A* **107**, 2124-2129 (2010).
16. William R. Harcombe *et al.*, Metabolic Resource Allocation in Individual Microbes Determines Ecosystem Interactions and Spatial Dynamics. *Cell Rep.* **7**, 1104-1115 (2014).
17. B. LaSarre, A. L. McCully, J. T. Lennon, J. B. McKinlay, Microbial mutualism dynamics governed by dose-dependent toxicity of cross-fed nutrients. *ISME J.* **11**, 337 (2016).
18. A. L. McCully, B. LaSarre, J. B. McKinlay, Recipient-biased competition for an intracellularly generated cross-fed nutrient is required for coexistence of microbial mutualists. *mBio* **8**, e01620-01617 (2017).

19. A. L. McCully, B. LaSarre, J. B. McKinlay, Growth-independent cross-feeding modifies boundaries for coexistence in a bacterial mutualism. *Env. Microbiol.* **19**, 3538-3550 (2017).
20. A. L. McCully *et al.*, An *Escherichia coli* nitrogen starvation response is important for mutualistic coexistence with *Rhodopseudomonas palustris*. *Appl. Environ. Microbiol.* **84**, e00404-00418 (2018).
21. M. Kim *et al.*, Need-based activation of ammonium uptake in *Escherichia coli*. *Mol. Sys. Biol.* **8**, 616 (2012).
22. A. Walter, J. Gutknecht, Permeability of small nonelectrolytes through lipid bilayer membranes. *J. Membr. Biol.* **90**, 207-217 (1986).
23. R. Dixon, D. Kahn, Genetic regulation of biological nitrogen fixation. *Nat. Rev. Microbiol.* **2**, 621-631 (2004).
24. J. B. McKinlay, C. S. Harwood, Carbon dioxide fixation as a central redox cofactor recycling mechanism in bacteria. *Proc. Natl. Acad. Sci. U S A* **107**, 11669-11675 (2010).
25. D. A. Lipson, The complex relationship between microbial growth rate and yield and its implications for ecosystem processes. *Front. Microbiol.* **6** (2015).
26. M. T. Wortel, E. Noor, M. Ferris, F. J. Bruggeman, W. Liebermeister, Metabolic enzyme cost explains variable trade-offs between microbial growth rate and yield. *PLOS Comput.l Biol.* **14**, e1006010 (2018).
27. C. Cheng *et al.*, Laboratory evolution reveals a two-dimensional rate-yield tradeoff in microbial metabolism. *PLOS Comput.l Biol.* **15**, e1007066 (2019).
28. J. S. McDowall *et al.*, Bacterial formate hydrogenlyase complex. *Proc. Natl. Acad. Sci. U S A* **111**, E3948-E3956 (2014).
29. A. A. Sangani, A. L. McCully, B. LaSarre, J. B. McKinlay, Fermentative *Escherichia coli* makes a substantial contribution to H_2 production in coculture with phototrophic *Rhodopseudomonas palustris*. *FEMS Microbiol. Lett.* **366**, fnz162 (2019).
30. D. P. Zimmer *et al.*, Nitrogen regulatory protein C-controlled genes of *Escherichia coli*: Scavenging as a defense against nitrogen limitation. *Proc. Natl. Acad. Sci. U S* **97**, 14674-14679 (2000).
31. A. Switzer, D. R. Brown, S. Wigneshweraraj, New insights into the adaptive transcriptional response to nitrogen starvation in Escherichia coli. *Biochem. Soc. Trans.* 10.1042/bst20180502, BST20180502 (2018).
32. P. Weglenski, A. J. Ninfa, S. Ueno-Nishio, B. Magasanik, Mutations in the glnG gene of *Escherichia coli* that result in increased activity of nitrogen regulator I. *J. Bacteriol.* **171**, 4479-4485 (1989).
33. R. Dixon, T. Eydmann, N. Henderson, S. Austin, Substitutions at a single amino acid residue in the nitrogen-regulated activator protein NTRC differentially influence its activity in response to phosphorylation. *Molec. Microbiol.* **5**, 1657-1667 (1991).
34. S. F. M. Hart, J. M. B. Pineda, C.-C. Chen, R. Green, W. Shou, Disentangling strictly self-serving mutations from win-win mutations in a mutualistic microbial community. *eLife* **8**:e44812 (2019).
35. A. J. Waite, W. Shou, Adaptation to a new environment allows cooperators to purge cheaters stochastically. *Proc. Natl. Acad. Sci. U S A* **109**, 19079-19086 (2012).

691 36. S. Estrela, J. J. Morris, B. Kerr, Private benefits and metabolic conflicts shape the
692 emergence of microbial interdependencies. *Environ. Microbiol.* **18**, 1415-1427
693 (2016).
694 37. O. M. Warsi, D. I. Andersson, D. E. Dykhuizen, Different adaptive strategies in *E.*
695 *coli* populations evolving under macronutrient limitation and metal ion limitation.
696 *BMC Evolutionary Biol.***18**, 72 (2018).
697 38. M.-K. Kim, C. S. Harwood, Regulation of benzoate-CoA ligase in
698 *Rhodopseudomonas palustris*. *FEMS Microbiol. Lett.* **83**, 199-203 (1991).
699 39. J. Quandt, M. F. Hynes, Versatile suicide vectors which allow direct selection for
700 gene replacement in Gram-negative bacteria. *Gene* **127**, 15-21 (1993).
701 40. K. A. Datsenko, B. L. Wanner, One-step inactivation of chromosomal genes in
702 *Escherichia coli K-12* using PCR products. *Proc. Natl. Acad. Sci. U S A* **97**, 6640-
703 6645 (2000).
704 41. F. E. Rey, Y. Oda, C. S. Harwood, Regulation of uptake hydrogenase and effects of
705 hydrogen utilization on gene expression in *Rhodopseudomonas palustris*. *J.*
706 *Bacteriol.* **188**, 6143-6152 (2006).
707 42. J. B. McKinlay, J. G. Zeikus, C. Vieille, Insights into *Actinobacillus succinogenes*
708 fermentative metabolism in a chemically defined growth medium. *Appl. Environ.*
709 *Microbiol.* **71**, 6651-6656 (2005).
710 43. J. J. Huang, E. K. Heiniger, J. B. McKinlay, C. S. Harwood, Production of hydrogen
711 gas from light and the inorganic electron donor thiosulfate by *Rhodopseudomonas*
712 *palustris*. *Appl. Environ. Microbiol.***76**, 7717-7722 (2010).
713 44. K. Zhou *et al.*, Novel reference genes for quantifying transcriptional responses of
714 *Escherichia coli* to protein overexpression by quantitative PCR. *BMC Molec. Biol.*
715 **12**, 18 (2011).
716 45. A. M. Bolger, M. Lohse, B. Usadel, Trimmomatic: a flexible trimmer for Illumina
717 sequence data. *Bioinformatics* **30**, 2114-2120 (2014).
718 46. D. E. Deatherage, J. E. Barrick, "Identification of Mutations in Laboratory-Evolved
719 Microbes from Next-Generation Sequencing Data Using breseq" in Engineering and
720 Analyzing Multicellular Systems: Methods and Protocols, L. Sun, W. Shou, Eds.
721 (Springer New York, New York, NY, 2014), 10.1007/978-1-4939-0554-6_12, pp.
722 165-188.
723 47. H. Li, R. Durbin, Fast and accurate short read alignment with Burrows–Wheeler
724 transform. *Bioinformatics* **25**, 1754-1760 (2009).
725 48. P. Cingolani *et al.*, A program for annotating and predicting the effects of single
726 nucleotide polymorphisms, SnpEff. *Fly* **6**, 80-92 (2012).
727 49. F. W. Larimer *et al.*, Complete genome sequence of the metabolically versatile
728 photosynthetic bacterium *Rhodopseudomonas palustris*. *Nat. Biotechnol.* **22**, 55-61
729 (2004).
730 50. K. Hayashi *et al.*, Highly accurate genome sequences of Escherichia coli K-12
731 strains MG1655 and W3110. *Molec. Syst. Biol.* **2**, 2006.0007 (2006).
732 51. R. Simon, U. Priefer, A. Pühler, A Broad Host Range Mobilization System for In
733 Vivo Genetic Engineering: Transposon Mutagenesis in Gram Negative Bacteria.
734 *Bio/Technology* **1**, 784-791 (1983).